THE JOURNAL OF PHYSICAL CHEMISTRY A
A JOURNAL OF THE AMERICAN CHEMICAL SOCIETY

pubs.acs.org/JPCA

Article

Ion–Molecule Rate Constants for Reactions of Sulfuric Acid with Acetate and Nitrate Ions

Published as part of The Journal of Physical Chemistry virtual special issue "Advances in Atmospheric Chemical and Physical Processes".

Sandra K. W. Fomete, Jack S. Johnson, Nanna Myllys, Ivo Neefjes, Bernhard Reischl, and Coty N. Jen*

Cite This: https://doi.org/10.1021/acs.jpca.2c02072

Read Online

ACCESS | Metrics & More | Article Recommendations | Supporting Information

ABSTRACT: Atmospheric nucleation from precursor gases is a significant source of cloud condensation nuclei in the troposphere and thus can affect the Earth's radiative balance. Sulfuric acid, ammonia, and amines have been identified as key nucleation precursors in the atmosphere. Studies have also shown that atmospheric ions can react with sulfuric acid to form stable clusters in a process referred to as ion-induced nucleation (IIN). IIN follows similar reaction pathways as chemical ionization, which is used to detect and measure nucleation precursors via atmospheric pressure chemical ionization mass spectrometers. The rate at which ions form clusters depends on the ion–molecule rate constant. However, the rate constant varies based on the ion composition, which is often not known in the atmosphere. Previous studies have examined ion–molecule rate constants for sulfuric acid and nitrate ions but not for other atmospherically relevant ions like acetate. We report the relative rate constants of ion–molecule reactions between nitrate and acetate ions reacting with sulfuric acid. The ion–molecule rate constant for acetate and sulfuric acid is estimated to be a factor of 1.9–2.4 times higher than that of the known rate constant for nitrate and sulfuric acid. Using quantum chemistry, we find that acetate has a higher dipole moment and polarizability than nitrate. This may contribute to an increase in the collision cross-sectional area between acetate and sulfuric acid and lead to a greater reaction rate constant than nitrate. The ion–molecule rate constant for acetate with sulfuric acid will help quantify the contribution of acetate ions to atmospheric ion-induced new particle formation.

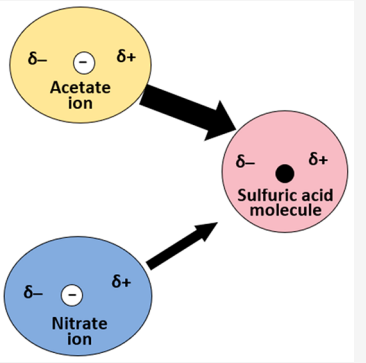

INTRODUCTION

Atmospheric new particle formation, which comprises of nucleation and subsequent particle growth, contributes to roughly 50% of the total number of global cloud condensation nuclei (CCN).[1−5] Clouds can either absorb or reflect incoming solar radiation to varying extents depending on cloud properties such as their lifetime and albedo, which are governed in part by CCN. As such, quantifying atmospheric nucleation rates is important to understand how aerosol particles affect clouds and the climate. Sulfuric acid is widely known to be a key player in new particle formation events in the atmosphere.[6−8] Basic gases such as ammonia and amines have also been shown to stabilize sulfuric acid clusters to form particles in the lower troposphere.[9−27] In the troposphere, ions produced from galactic cosmic rays have been predicted to enhance sulfuric acid nucleation in a process known as ion-induced nucleation (IIN).[10,28−31] Specifically, observations from the CERN CLOUD (Cosmic Leaving OUtdoor Droplets) chamber showed that negative ions, such as bisulfate, can enhance neutral sulfuric acid-ammonia nucleation rates by up to a factor of 5 in the upper troposphere.[10] Many other ions are present in the atmosphere and will likely help nucleate sulfuric acid clusters at different rates depending on their abundance and composition. Hence, understanding the interactions between atmospherically relevant ions and sulfuric acid clusters is important in understanding NPF in the atmosphere.

Acetic acid (CH_3COOH) is one of the most prevalent carboxylic acids in the atmosphere and is present in rural, urban, and marine environments in the low-ppbv range.[32−36] Acetic acid is released into the atmosphere from various sources such as biomass burning,[32] automobile exhaust,[37] and biogenic emissions.[38,39] Studies have shown that over 90% of the total acetic acid concentration in aerosols is present in the gas-phase.[35,40−43] In addition, gas-phase nitrate ions (NO_3^-, $HNO_3{\cdot}NO_3^-$, or $H_2O{\cdot}NO_3^-$) formed via a variety of pathways from HNO_3 and NO_x emissions have also been observed at

Received: March 25, 2022
Revised: October 12, 2022

pptv levels in the atmosphere.[44−46] Hence, acetate and nitrate ions could play important roles in atmospheric IIN depending on their concentrations and ionization rate constants.

IIN reaction pathways are also similar to how electrically neutral sulfuric acid clusters are typically measured using atmospheric pressure chemical ionization mass spectrometers (CIMS).[11,13,15,23,47] Many nucleation studies using a CIMS have employed nitrate ($(HNO_3)_{0-2}\cdot NO_3^-$) as the reagent ion to ionize and measure clusters. Acetate has also been used to ionize and detect atmospherically relevant organic acids and more aminated sulfuric acid clusters.[48,49] The concentration of sulfuric acid and its freshly nucleated clusters can be calculated by ratioing their respective mass spectrometer signals to that of the reagent ions. Two approaches have been used in literature for calculating the concentration of sulfuric acid from measured CIMS signals: (1) a kinetic approach, which uses the ionization rate laws and the ion−molecule collision rate constants between the reagent ion and the neutral sulfuric acid molecules,[11,13,48,50,51] and (2) a calibration approach, which requires a known amount of sulfuric acid to be generated.[52]

The kinetic and calibration methods are used for calculating sulfuric acid concentrations from measured mass spectrometer signals. To convert measured mass spectrometer signals to actual concentrations using the calibration method, a calibration factor is needed. Obtaining this calibration constant for sulfuric acid monomer is straightforward with a constant source of sulfuric acid vapor. However, it is challenging to obtain calibration constants for the wide range of sulfuric acid clusters that could form via nucleation in the atmosphere. As such, calculating concentrations of sulfuric acid clusters using the calibration method is limited due to the inability to produce and measure calibration constants for all cluster types. The calibration method which has previously been explained by Berresheim et al.[50] has no explicit value for ionization rate constants and ionization reaction times as these are captured in the calibration constant. Thus, cluster concentrations obtained using the calibration method have uncertainties associated with unknown ionization reaction times and ionization rate constants that are grouped into the calibration factor. For the kinetic approach, the ionization reaction time is determined by the electric field strength driving ions into the CIMS, reagent ion mobility, and mass spectrometer inlet dimensions.[51] Hence, the only unknown factor in the kinetic approach is the ionization rate constant, which is typically assumed to be the collisional rate constant between the reagent ion and the nucleated clusters.[11,48] Previous measurements indicate that the rate constant for nitrate and sulfuric acid is the collision rate constant, which equals 1.9×10^{-9} cm^3 s^{-1}.[53,54] The ionization rate constant for acetate ions with sulfuric acid molecules is unknown.

The purpose of this study is to determine the ionization rate constant for acetate ions with sulfuric acid. Previous studies using acetate reagent ions have assumed the ion−molecule rate constant for acetate and sulfuric acid to be equal to that of nitrate with sulfuric acid.[48] To evaluate this assumption, the relative rate constant for acetate reaction with sulfuric acid was measured relative to the known nitrate rate constant with sulfuric acid. Two identical, clean sulfuric acid flow reactors with highly reproducible conditions were each connected in-line with custom-built nitrate/acetate atmospheric pressure chemical ionization (1) long time-of-flight mass spectrometer (Pittsburgh Cluster CIMS, PCC) and (2) quadrupole mass spectrometer (Minnesota Cluster CIMS, MCC).[11,13,55] The measured acetate rate constant obtained from the PCC and MCC was compared with the rate constant calculated from ion−molecule collision theory. Note, temperature effects were not examined, and the relative ion−molecule rate constants presented in this study only apply at 303 K. The presented acetate ionization rate constant will enable more accurate measurements of sulfuric acid clusters using a CIMS and improve current models used to predict the rate of ion-induced nucleation in the atmosphere.

EXPERIMENTAL METHODS

Two identical laminar flow reactors were used to produce a constant concentration of gaseous sulfuric acid. Details of these flow reactors are given in Fomete et al.[56] with important parameters provided here. The flow reactors were operated at atmospheric pressure, 20% RH, and 303 K. Sulfuric acid vapor is produced by flowing nitrogen gas over a temperature-controlled reservoir containing liquid sulfuric acid (99.999% based on trace metal analysis, MilliporeSigma) and injected into the top of the flow reactor. A constant sulfuric acid concentration was achieved in the reactor by maintaining a given flow rate of gaseous sulfuric acid with a constant total flow of either 4.5 or 4.0 sLpm (see the Supporting Information, Figure S1).

Two chemical ionization mass spectrometers (CIMS) were used to measure sulfuric acid. The Pittsburgh Cluster CIMS (PCC) contains a custom-built transverse atmospheric pressure chemical ionization inlet with two quadrupoles to focus the ion beam and a long time-of-flight mass filter.[55] The Minnesota Cluster CIMS (MCC) includes another custom-built transverse atmospheric pressure chemical ionization inlet with dimensions and geometries that vary from PCC. This results in different inlet electric fields between the PCC and MCC. In addition, the MCC contains a conical octupole followed by a quadrupole mass filter.[11,13]

The PCC and MCC were each connected in-line with a sulfuric acid flow reactor to minimize sampling losses.[13,55] For both the PCC and MCC, reagent ions were produced by passing nitrogen over liquid acetic acid (≥99.7% MilliporeSigma, diluted to 60% v/v in HPLC-grade water) or nitric acid (69.3% Fisher Chemical) and then over ^{210}Po (model 1U200, NRD). The holder containing the ^{210}Po strip was shielded with a stainless-steel plate to prevent alpha particles from escaping into the reactor's flow and ionizing sulfuric acid. The acetate reagent ions measured by the PCC included $H_2O\cdot CH_3CO_2^-$ (~1×10^3 Hz), $CH_3CO_2H\cdot CH_3CO_2^-$ (~6×10^3 Hz), and $CH_3CO_2^-$ (~1×10^5 Hz). For nitrate, the resulting ions measured by the PCC included NO_3^- (~1×10^5 Hz), $HNO_3\cdot NO_3^-$ (~2×10^5 Hz), and $(HNO_3)_2\cdot NO_3^-$ (~4×10^2 Hz). Meanwhile, the acetate reagent ions measured by the MCC included $H_2O\cdot CH_3CO_2^-$ (~70×10^3 Hz), $CH_3CO_2H\cdot CH_3CO_2^-$ (~2×10^3 Hz), and $CH_3CO_2^-$ (~20×10^3 Hz). For nitrate, the resulting ions measured by the MCC included NO_2^- (~8×10^3 Hz), $HNO_3\cdot NO_3^-$ (~2×10^5 Hz), and $(HNO_3)_2\cdot NO_3^-$ (~3×10^3 Hz). The abundances of these reagent ions follow their computed binding free energies with $HNO_3\cdot NO_3^-$ having a binding energy of −21.7 kcal/mol, $CH_3CO_2H\cdot CH_3CO_2^-$ of −17.8 kcal/mol, and $H_2O\cdot CH_3CO_2^-$ of −8.3 kcal/mol (DLPNO−CCSD(T)/aug-cc-pVTZ/wB97X-D/6-31++G** at 298.15 K).

The neutral sulfuric acid monomer (H_2SO_4) and dimers ($(H_2SO_4)_2$) in the sample flow were chemically ionized by either acetate or nitrate ions and measured by the PCC and

https://doi.org/10.1021/acs.jpca.2c02072
J. Phys. Chem. A XXXX, XXX, XXX−XXX

MCC in negative ion mode. The inlet flows and voltage tuning parameters for each instrument were held constant between nitrate and acetate experiments. Chemical ionization of sulfuric acid clusters by nitrate or acetate depends on the chemical ionization reaction time (t_{CI}). This t_{CI} is a function of the dimensions of the PCC or MCC inlet, the electric field strength driving ions into the mass spectrometer, and the mobility of the reagent ions (see Supporting Information). Varying the voltages in the atmospheric pressure inlet alters the electric field strength and thus t_{CI} between the reagent ion and the sample flow. Time-dependent ion processes such as ion-induced clustering (IIC) and ion decomposition can be probed in the PCC or MCC inlet by varying t_{CI}.[11,13,48,51]

In this study, two types of experiments were conducted using the PCC and MCC: (1) At constant t_{CI}, the sulfuric acid concentration ($[H_2SO_4]$) in the reactor was varied and (2) At a given $[H_2SO_4]$, t_{CI} was varied. Each type of experiment was performed using nitrate and acetate as reagent ions. The rate constant for chemical ionization of sulfuric acid by acetate was determined when t_{CI} was held constant while sulfuric acid concentrations in the flow reactor were varied. The ion-induced clustering (IIC) rate constant of charged sulfuric monomer (bisulfate) with neutral sulfuric acid was obtained by varying t_{CI} at a fixed sulfuric acid concentration in the reactor. The determined IIC rate constant confirmed the estimated ionization rate constant for acetate and sulfuric acid.

RESULTS AND DISCUSSION

The ion−molecule/cluster reactions that can occur between nitrate/acetate and H_2SO_4 and $(H_2SO_4)_2$ are shown below. Note, the nitrate dimer ($HNO_3{\cdot}NO_3^-$) is the dominant reagent ion for the PCC and MCC. The acetate monomer ($CH_3CO_3^-$) is the main ion for the PCC whereas acetate with water ($CH_3CO_2^-{\cdot}H_2O$) is the dominant reagent ion for the MCC. It is likely that acetate with water is the main ionizing ion in the PCC but fragments in the vacuum region. Ions experience more fragmentation in the PCC as evidenced by the larger fraction of nitrate compared to nitrate dimer signals (50%) compared to 4% for the MCC. The below ionization reactions are therefore written for the nitrate dimer and acetate with waters.

Nitrate−Sulfuric Acid.

$$H_2SO_4 + HNO_3{\cdot}NO_3^- \xrightarrow{k_{1,\text{nitrate}}} HSO_4^-{\cdot}HNO_3 + HNO_3 \quad \text{(R1)}$$

$$(H_2SO_4)_2 + HNO_3{\cdot}NO_3^- \xrightarrow{k_{2,\text{nitrate}}} H_2SO_4{\cdot}HSO_4^- + 2HNO_3 \quad \text{(R2)}$$

Acetate−Sulfuric Acid.

$$H_2SO_4 + CH_3CO_2^-{\cdot}H_2O \xrightarrow{k_{1,\text{acetate}}} HSO_4^- + CH_3CO_2H + H_2O \quad \text{(R3)}$$

$$(H_2SO_4)_2 + CH_3CO_2^-{\cdot}H_2O \xrightarrow{k_{2,\text{acetate}}} H_2SO_4{\cdot}HSO_4^- + CH_3CO_2H + H_2O \quad \text{(R4)}$$

Ion-Induced Clustering (IIC) Reactions.

$$H_2SO_4 + HSO_4^-{\cdot}HNO_3 \xrightarrow{k_{21,\text{nitrate}}} H_2SO_4{\cdot}HSO_4^- + HNO_3 \quad \text{(R5)}$$

$$H_2SO_4 + HSO_4^- \xrightarrow{k_{21,\text{acetate}}} H_2SO_4{\cdot}HSO_4^- \quad \text{(R6)}$$

Reactions R5 and R6 represent the ion-induced clustering reactions whereby a charged sulfuric acid monomer ($HSO_4^-{\cdot}HNO_3$ or HSO_4^-) ionizes another neutral sulfuric acid monomer (H_2SO_4). This and previous studies have measured most sulfuric acid monomer ions with nitrate as $HSO_4^-{\cdot}HNO_3$.[11,48] The only measured sulfuric acid monomer with acetate is HSO_4^-. It is likely that the $HSO_4^-{\cdot}CH_3CO_2H$ is unstable and the acetic acid ligand quickly evaporates. In addition, neutral sulfuric acid monomers and dimers could contain ligands such as water which are lost from these clusters during measurement.[50,57] The chemical ionization rate constant has previously been measured to be $k_{1,\text{nitrate}} = 1.9 \times 10^{-9}$ cm^3 s^{-1} and was estimated to equal the ion-induced rate constant, $k_{21,\text{acetate}}$.[28,53,54] $k_{2,\text{nitrate}}$ is assumed to be 2×10^{-9} cm^3 s^{-1} from collision theory.[58,59] The acetate rate constants, $k_{1,\text{acetate}}$, $k_{21,\text{acetate}}$, and $k_{2,\text{acetate}}$, have not previously been measured.

Given the elementary reactions shown in reactions R1 and R3, rate expressions for the formation/depletion of the reagent ions $HNO_3{\cdot}NO_3^-$ and $CH_3CO_2^-{\cdot}H_2O$ as well as HSO_4^- and $H_2SO_4{\cdot}HSO_4^-$ can be solved with respect to t_{CI}, the chemical ionization reaction time, to obtain the neutral sulfuric acid monomer and dimer concentrations (see the Supporting Information).[48,50] For the first set of PCC experiments, t_{CI} was held constant (nitrate was 28 ms and acetate 26 ms) while sulfuric acid concentration was varied in the reactor. Meanwhile for the MCC experiments, t_{CI} was kept constant at 20 ms for nitrate and 19 ms for acetate. Uncertainty in the calculated t_{CI} could arise due to nonidealities in the assumed parallel plate electric field in the PCC and MCC inlets. However, any systematic uncertainties in the calculated t_{CI} will not affect the rate constants determined in this study as the same inlet electric fields and flow rates were used for the nitrate and acetate experiments. The concentration of H_2SO_4, ($[H_2SO_4]$) can be calculated from the signal ratio of HSO_4^- to the reagent ion signal (see Supporting Information) and is shown below:

$$\frac{S_{\text{sulfuric acid monomer}}}{S_{\text{reagent}}} = z_i k_1 [H_2SO_4] t_{CI} \quad (1)$$

Equation 1 is similar for both nitrate and acetate where the rate constant, k_1, is either $k_{1,\text{nitrate}}$ or $k_{1,\text{acetate}}$, z_i is the factor describing the mass-dependent transmission efficiency (MTE) of the measured sulfuric acid ion relative to either the weighted average of the observed acetate or nitrate reagent ions. The MCC has a known MTE curve which was previously measured by Jen et al., and the PCC's MTE curve was estimated from the absolute transmission of Heinritzi et al.[60,61] $S_{\text{sulfuric acid monomer}}$ is the sum of the signals at 160 m/z and 97 m/z (i.e., S_{97+160}) for nitrate. For acetate, $S_{\text{sulfuric acid monomer}}$ is the bisulfate ion signal at m/z 97 (i.e., S_{97}) only since there were no observed sulfuric acid molecules clustered to acetate ions for either instrument. S_{reagent} for nitrate is the sum of the signals at 62 m/z (NO_3^-), 125 m/z ($HNO_3{\cdot}N_3^-$), and 188 m/z ($(HNO_3)_2{\cdot}NO_3^-$)) which will be denoted as S_{nitrate}. For acetate, S_{reagent} is the sum of the signals at 59 m/z ($CH_3CO_2^-$), 77 m/z ($H_2O{\cdot}CH_3CO_2^-$), and 119 m/z ($CH_3CO_2H{\cdot}CH_3CO_2^-$) and is denoted as S_{acetate}. Given that chemical ionization of sulfuric acid is driven mostly by the most abundant reagent ion, it is reasonable to assume one rate constant characterizing the

https://doi.org/10.1021/acs.jpca.2c02072
J. Phys. Chem. A XXXX, XXX, XXX−XXX

dominant reagent ion. The formation rate of HSO_4^- from chemical ionization of H_2SO_4 with reagent ion is much faster than the rate at which HSO_4^- is lost via IIC to H_2SO_4. Hence, eq 1 assumes negligible losses of HSO_4^- via IIC and constant reagent ion concentration. In addition, the flow reactor contained almost no neutral sulfuric acid dimers and larger clusters as these are only present with other stabilizing bases and other contaminant species.[11] Absence of these larger sulfuric acid clusters leads to negligible formation of HSO_4^- and $H_2SO_4{\cdot}HSO_4^-$ from the decomposition of larger ion clusters.

Figure 1 shows the signal ratio $S_{97}/S_{acetate}$ plotted against $S_{97+160}/S_{nitrate}$ with varying $[H_2SO_4]$ and constant $t_{CI} \sim 26-28$ ms for the PCC (red) and constant $t_{CI} \sim 19-20$ ms for the MCC (black). Each point for the PCC measurements represents a six-day average of the signal ratios at a given sulfuric flow rate/concentration in the flow reactor whereas the points for the MCC represent a three-day average. Plotting $S_{sulfuric\ acid\ monomer}/S_{reagent}$ versus t_{CI} shown in eq 1 yields a slope equivalent to $k_1[H_2SO_4]$. Thus, the ratio of $S_{97+160}/S_{nitrate}$ to $S_{97}/S_{acetate}$ derived from the nitrate and acetate expressions of eq 1 yields $k_{1,nitrate}/k_{1,acetate}$. The linear relationship between $S_{97}/S_{acetate}$ vs $S_{97+160}/S_{nitrate}$ corrected for MTE shows a slope of 2.4 for the PCC and a slope of 1.9 for the MCC each with a near zero y-intercept (solid lines). For the case where $z_i = 1$ (dashed lines shown in Figure 1), the slope of $S_{97}/S_{acetate}$ vs $S_{97+160}/S_{nitrate}$ is 2.4 for both the PCC and MCC. A slope of 1.9−2.4 implies that the ionization rate constant of acetate ions is 1.9−2.4 times greater than that of the nitrate collision rate constant with sulfuric acid at $T = 303$ K. Therefore, the acetate rate constant with sulfuric acid is 1.9 to 1.4 times greater the previously measured[53] $k_{1,nitrate} = 1.9 \times 10^{-9}$ cm^3 s^{-1} with $k_{1,acetate}$ estimated to be $(3.6-4.6) \times 10^{-9}$ cm^3 s^{-1}.

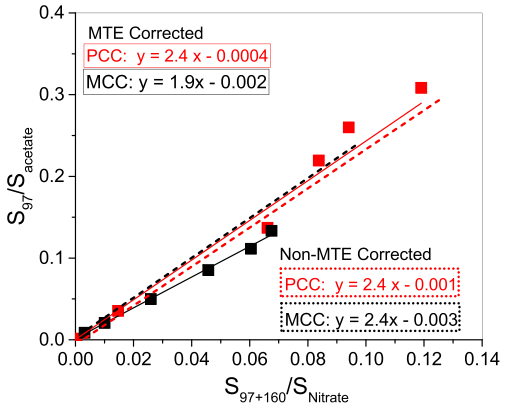

Figure 1. Plot of the sulfuric acid monomer to reagent signal ratios for acetate ($S_{97}/S_{acetate}$) vs the monomer to reagent signal ratio for nitrate ($S_{97+160}/S_{nitrate}$). A linear fit of the MTE-corrected signal ratios reveals slopes of 2.4 and 1.9 respectively for the PCC (solid red line) and MCC (solid black line). The PCC and MCC signal ratios not corrected for MTE (red and black dashed lines respectively) have a slope of 2.4.

The range of $k_{1,acetate}$ reflects the uncertainty in the MTE curves for the MCC and PCC. Only two calibration points exist for the MTE curves in the mass range of interest (59−195 m/z).[13,60,61] In addition, slight differences in inlet configuration, electric field, and flow rates compared to the MTE calibration setup will impact the transmission efficiency. Regardless, the MCC and PCC still observe a factor of 1.9−2.4 times higher for $k_{1,acetate}$ compared to $k_{1,nitrate}$ despite major instrumentation differences. This strongly indicates that acetate ionizes sulfuric acid faster than nitrate given the equivalent concentrations.

With a known ionization rate constant, $[H_2SO_4]$ in the flow reactor can be obtained from the monomer and reagent ion signals (eq 1). Figure 2 shows $[H_2SO_4]$ measured with nitrate and acetate at different sulfuric acid flow rates injected into the reactors connected to PCC and MCC averaged over a period of six and three days, respectively. Correcting the PCC measured $[H_2SO_4]$ with $k_{1,acetate} = 4.6 \times 10^{-9}$ cm^3 s^{-1} yields a better agreement of $[H_2SO_4]$ measured with nitrate and acetate as shown in Figure 2A. With the corrected $k_{1,acetate}$, there is only a ∼ 25% difference between $[H_2SO_4]$ measured with acetate and nitrate compared to a ∼ 70% difference when $k_{1,acetate}$ is assumed to be equal to $k_{1,nitrate}$. For the MCC, $k_{1,acetate} = 3.6 \times 10^{-9}$ cm^3 s^{-1} produces measured $[H_2SO_4]$ with less than 15% difference compared to nitrate and is shown in Figure 2B. The largest difference in $[H_2SO_4]$ is seen at low

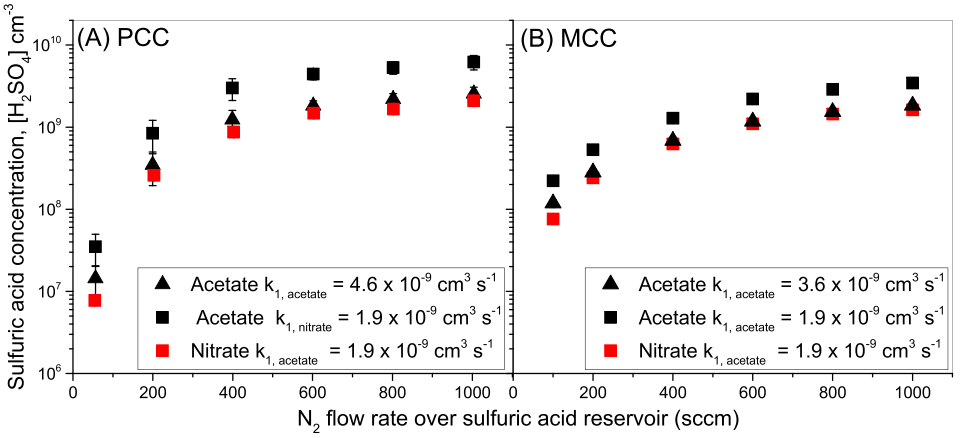

Figure 2. Calculated sulfuric acid monomer concentration $[H_2SO_4]$ vs flow rate of sulfuric acid injected in two different flow reactors for acetate (black) and nitrate (red). (A) Squares show $[H_2SO_4]$ calculated with $k_{1,acetate} = k_{1,nitrate} = 1.9 \times 10^{-9}$ cm^3 s^{-1} for PCC measurements. Triangles are $[H_2SO_4]$ calculated with $k_{1,acetate} = 4.6 \times 10^{-9}$ cm^3 s^{-1}. (B) Squares show $[H_2SO_4]$ calculated with $k_{1,acetate} = k_{1,nitrate} = 1.9 \times 10^{-9}$ cm^3 s^{-1} for MCC measurements. Triangles are $[H_2SO_4]$ calculated with $k_{1,acetate} = 3.6 \times 10^{-9}$ cm^3 s^{-1}. The error bars show the extent to which the sulfuric acid concentrations varied for a given sulfuric acid flow rate over the 6-day and 3-day measurement periods for the PCC and MCC, respectively.

https://doi.org/10.1021/acs.jpca.2c02072
J. Phys. Chem. A XXXX, XXX, XXX−XXX

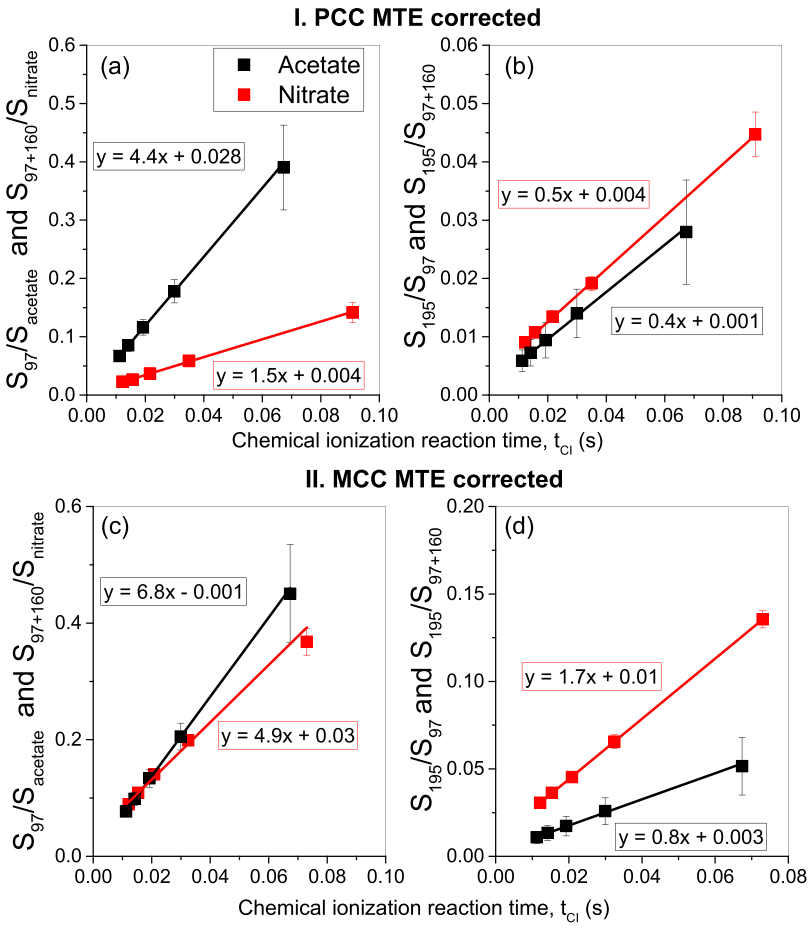

Figure 3. Panels a and c show MTE-corrected signal ratios of sulfuric acid monomer to the reagent ($S_{97}/S_{acetate}$ and $S_{97+160}/S_{nitrate}$) vs t_{CI} at constant sulfuric acid concentration for acetate (black) and nitrate (red) for PCC and MCC respectively. Panels b and d show MTE-corrected signal ratios of the sulfuric acid dimer to the monomer (S_{195}/S_{97} and S_{195}/S_{97+160}) vs t_{CI} for acetate (black) and nitrate (red) for PCC and MCC, respectively. The lines are linear fits, and the error bars show the extent to which the signal ratios at a given t_{CI} varied over the measurement period.

sulfuric acid flow rates and is likely due to difficulty in maintaining a consistent low flow rate over the sulfuric acid reservoir.

The IIC rate constant for the formation of sulfuric acid dimers is also examined to validate the estimated $k_{1,acetate}$. Sulfuric acid dimer ions measured by the PCC and MCC are primarily formed by IIC of a H_2SO_4 with HSO_4^- due to negligible concentration of neutral sulfuric dimers in the flow reactor. IIC reactions between charged and neutral sulfuric acid molecules (reactions R5 and R6) for nitrate and acetate can be probed by varying t_{CI} at constant sulfuric acid concentration. The IIC rate constant for the formation of sulfuric acid dimers using nitrate and acetate reagents, $k_{21,acetate}$ and $k_{21,acetate}$, respectively, could differ from each other depending on if HSO_4^- has a ligand attached to it and the identity of this ligand.

As shown in the Supporting Infomation, the rate expression for the formation of $H_2SO_4{\cdot}HSO_4^-$ from reactions R5 and R6 can be integrated at short t_{CI} to obtain an expression in terms of dimer and monomer−ion signal ratios as shown below:

$$\frac{S_{\text{sulfuric acid dimer}}}{S_{\text{sulfuric acid monomer}}} = z_j\left(\frac{k_2}{k_1}\frac{[(H_2SO_4)_2]}{[H_2SO_4]} + \frac{1}{2}k_{21}[H_2SO_4]t_{CI}\right) \quad (2)$$

Here k_{21} is the IIC rate constant, k_2 is the sulfuric acid dimer ionization rate constant, k_1 is the sulfuric acid monomer ionization rate constant, and z_j is the MTE between the sulfuric acid dimer and monomer. $S_{\text{sulfuric acid dimer}}$ is measured by the PCC and MCC at m/z 195 and will therefore be subsequently denoted as S_{195}. eq 2 assumes negligible formation of dimer ions from ion decomposition of larger clusters, constant reagent ion concentration, and constant $[H_2SO_4]$ and $[H_2SO_4]_2$ during the chemical ionization.

Panels a and b of Figure 3 illustrate the MTE-corrected ratios of sulfuric acid monomer to reagent signals ($S_{97}/S_{acetate}$ and $S_{97+160}/S_{nitrate}$) as a function of t_{CI} and the ratio of sulfuric acid dimer to monomer−ion signal (S_{195}/S_{97} and S_{195}/S_{97+160}) vs t_{CI}, respectively, measured with the PCC. Similarly, panels c and d of Figures 3 illustrate MTE-corrected $S_{97}/S_{acetate}$ and $S_{97+160}/S_{nitrate}$ vs t_{CI} along with S_{195}/S_{97} and S_{195}/S_{97+160} vs t_{CI} for the MCC. Note, the PCC measurements are 6-day averages and the MCC measurements are 4-day averages. Dividing the slope of the lines in panels a and c of Figure 3 to the corresponding slopes in panels b and d of Figure 3 yields $\frac{2k_1}{k_{21}}$ (see Supporting Information). Using this IIC approach to calculate $k_{1,nitrate}$ eliminates any systematic uncertainties in the calculated t_{CI} which could arise from uncertainties in ion mobilities and imperfections in electric field as this approach is independent of the exact t_{CI} used for acetate and nitrate. For the PCC, the ratio $\frac{2k_1}{k_{21}}$ is 10.8 and 6.0 for acetate and 3.4 and 2.5 for nitrate with and without MTE correction, respectively.

https://doi.org/10.1021/acs.jpca.2c02072
J. Phys. Chem. A XXXX, XXX, XXX−XXX

In addition, the MCC ratio $\frac{2k_1}{k_{21}}$ is 9.1 and 5.3 for acetate and 2.9 and 2.6 for nitrate with and without MTE correction, respectively. See the Supporting Information for PCC and MCC slope ratios obtained when signals were not corrected for MTE. These results demonstrate two potential conclusions: (1) Assuming $k_{1,acetate} = (1.9–2.4) \times k_{1,nitrate}$ (from above), then $k_{21,nitrate} = (1.1–1.3) \times 10^{-9}$ cm^3 s^{-1} and $k_{21,acetate} = 8 \times 10^{-10}$ to 2×10^{-9} cm^3 s^{-1}. (2) Assuming that IIC occurs at the collision limit such that $k_{21,nitrate} = k_{21,acetate} = 1.9 \times 10^{-9}$ cm^3 s^{-1}, then $k_{1,acetate}$ is approximately a factor of 2–3 higher than $k_{1,nitrate}$. The estimated ion–molecule rate constants reported in this study are summarized in Table 1. Note, $k_{21,acetate}$ agrees with the collision rate constant of 1.9×10^{-9} cm^3 s^{-1} when z_j is assumed to be 1 (i.e., when the sulfuric acid dimer and monomer have similar transmission efficiencies). Also, the $k_{1,acetate}$ better matches the previously estimated factor of (1.9–2.4) $\times$ $k_{1,nitrate}$ when $z_j = 1$. This suggests that the MTE values of the sulfuric acid dimer (195 m/z) for both the PCC and MCC may be too high. Overall, this additional experimental approach with variations in t_{CI} provides further evidence that $k_{1,acetate}$ is (1.9–2.4) $\times$ $k_{1,nitrate}$.

Table 1. Summary of Estimated Ion–Molecule Rate Constants at T = 303 K and RH = 20%

	ion–molecule rate constant (cm^3 s^{-1})
$k_{1,nitrate}$[a]	1.9×10^{-9}
$k_{1,acetate}$	$(3.6–4.6) \times 10^{-9}$
$k_{21,nitrate}$	1.1×10^{-9} to 1.3×10^{-9}
$k_{21,acetate}$	8×10^{-10} to 2×10^{-9}

[a]Collision rate constant previously measured by Viggiano et al.[53]

A slope ratio $\frac{2k_1}{k_{21}}$ close to 2 suggests that $k_{21,nitrate} = k_{1,nitrate}$. However, the MTE-corrected slope ratios for the PCC mentioned above were about 3.4 and 2.5 when not corrected for MTE. The MCC exhibited slope ratios of 2.6 and 2.9 when not MTE corrected. Jen et al. suggest that a slope ratio higher than 2 indicates a potential contamination in the flow reactor.[61] However, the values of the y-intercept in this study for S_{195}/S_{97} and S_{195}/S_{97+160} vs t_{CI} for acetate and nitrate, respectively, in Figure 3, panels b and d, are almost zero which suggests a near zero concentration of neutral sulfuric acid dimers (eq 2). This implies that the flow reactors were free of stabilizing compounds that would allow the formation of the neutral sulfuric acid dimer.[11,48] In addition, any uncertainty in the calculated t_{CI} values in Figure 3 would not affect the slope ratio since this uncertainty will affect each individual slope to the same extent. The largest uncertainty in the calculated t_{CI} likely occurs at the lower t_{CI} where any imperfections in the parallel plate electric field in the mass spectrometer inlets would significantly bias the drift time for ions.

Current ion–molecule collision theories, such as average dipole orientation (ADO)[62] or angular momentum average dipole orientation (AADO),[63] do not capture the experimentally determined factor of 1.9–2.4 difference between acetate and nitrate with sulfuric acid. For example, ADO predicts acetate and nitrate to have similar collision rate constants with sulfuric acid such that $k_{1,nitrate} = k_{1,acetate} = 2 \times 10^{-9}$ cm^3 s^{-1}. This is due to acetate and nitrate having comparable reduced masses with respect to sulfuric acid.[64] Specifically, ADO treats an ion as a point charge which then induces a dipole moment in the molecule.[64,65] In contrast, the acetate ions, including acetic acid and water ligands, have significant dipole moments and polarizabilities compared to nitrate. The dipole moments of $CH_3CO_2^-$, $CH_3CO_2^-\cdot H_2O$, and $CH_3CO_2H\cdot CH_3CO_2^-$ (4.03, 4.24, and 3.93 D, respectively) are more than 3 times greater those that of NO_3^- and $HNO_3\cdot NO_3^-$ (0 and 1.3 D, respectively). The polarizability of $CH_3CO_2^-$, $CH_3CO_2^-\cdot H_2O$, and $CH_3CO_2H\cdot CH_3CO_2^-$ (6.03, 7.00, and 10.7 Å^3, respectively) are also greater than that of NO_3^- and $HNO_3\cdot NO_3^-$ (4.08 and 7.88 Å^3 respectively). These dipole and polarizability values were calculated from computational chemistry using the ωB97X-D/6-31++G** level of theory and summarized in Table S2.[66]

Similar to when an ion is treated as a point charge, the ion's dipole will also induce a dipole in the neutral molecule. However, this system now contains four partial charges, two from the ion's permanent dipole moment and two from the induced dipole of the molecule. Note, sulfuric acid also has a dipole moment. The additional charge interaction, including dipole–dipole, ion-induced dipole, and ion–molecule, could contribute to a higher force between the ion and molecule. This would expand the collision cross-sectional area and result in a higher rate constant.

To the best of our knowledge, no previous study has developed a theory that further includes the effect of an ion's dipole and polarizability on the collision rate constant of nitrate and acetate ions with sulfuric acid. Eichelberger et al. showed that while many ion–molecule reactions can be approximated such that the ion is a point charge, an additional attractive potential should be considered when the ion is highly polarizable compared to the neutral molecule.[67] This additional attractive potential between the ion and the neutral molecule increased the collision cross-sectional area and alter the angle of collision between the ion and neutral molecule. Furthermore, preliminary molecular dynamic simulations following Neefjes et al.[68] suggest a higher collision rate constant for acetate ions (with and without water ligand) with sulfuric acid compared to nitrate dimer ion due in part to acetate's dipole moment. A forthcoming molecular dynamic simulation study will examine the role ion's dipole and composition play on collision rate constants with molecular dipoles.

CONCLUSION

In this study, the relative ionization rate constant of sulfuric acid with acetate ions was determined to be 1.9–2.4 times higher than with nitrate ions at 303 K and 20% RH. This results in an ionization rate constant of $(3.6–4.6) \times 10^{-9}$ cm^3 s^{-1} for sulfuric acid with acetate. The IIC rate constant between charged sulfuric acid monomer and neutral sulfuric acid monomer was also determined in order to confirm the observed $k_{1,acetate}$. The higher rate constant of acetate with sulfuric acid compared to nitrate may be due to the higher dipole moment and polarizability of the acetate ions compared to nitrate. The additional dipole on the ion could contribute to the interaction force between the ion and molecule which would increase the collision cross-sectional area and thus ion–molecule rate constant. Combined, these results demonstrate how ion composition impacts the rate at which ion-induced nucleation occurs and ultimately influences atmospheric aerosol number concentrations.

https://doi.org/10.1021/acs.jpca.2c02072
J. Phys. Chem. A XXXX, XXX, XXX–XXX

■ ASSOCIATED CONTENT

Supporting Information

The Supporting Information is available free of charge at https://pubs.acs.org/doi/10.1021/acs.jpca.2c02072.

Additional details for daily baseline measurements, rate equations for nitrate, acetate, and sulfuric acid monomer, and calculated *xyz* coordinates for stable nitrate and acetate ions (PDF)

■ AUTHOR INFORMATION

Corresponding Author

Coty N. Jen − *Department of Chemical Engineering, Carnegie Mellon University, Pittsburgh, Pennsylvania 15213, United States; Center for Atmospheric Particle Studies, Carnegie Mellon University, Pittsburgh, Pennsylvania 15213, United States;* orcid.org/0000-0002-3633-4614; Email: cotyj@andrew.cmu.edu

Authors

Sandra K. W. Fomete − *Department of Chemical Engineering, Carnegie Mellon University, Pittsburgh, Pennsylvania 15213, United States; Center for Atmospheric Particle Studies, Carnegie Mellon University, Pittsburgh, Pennsylvania 15213, United States;* orcid.org/0000-0002-1393-5353

Jack S. Johnson − *Department of Chemical Engineering, Carnegie Mellon University, Pittsburgh, Pennsylvania 15213, United States; Center for Atmospheric Particle Studies, Carnegie Mellon University, Pittsburgh, Pennsylvania 15213, United States;* orcid.org/0000-0001-6291-9467

Nanna Myllys − *Department of Chemistry, University of Jyväskylä, FI-40014 Jyväskylä, Finland; Department of Chemistry, Faculty of Science, University of Helsinki, FI-00014 Helsinki, Finland;* orcid.org/0000-0003-0384-7277

Ivo Neefjes − *Institute for Atmospheric and Earth System Research/Physics, Faculty of Science, University of Helsinki, FI-00014 Helsinki, Finland;* orcid.org/0000-0003-4549-0114

Bernhard Reischl − *Institute for Atmospheric and Earth System Research/Physics, Faculty of Science, University of Helsinki, FI-00014 Helsinki, Finland;* orcid.org/0000-0001-7333-4923

Complete contact information is available at: https://pubs.acs.org/10.1021/acs.jpca.2c02072

Notes

The authors declare no competing financial interest.

■ ACKNOWLEDGMENTS

S.K.W.F., J.S.J., and C.N.J. acknowledge funding from NSF AGS-1913504. S.K.W.F. also acknowledges support from a CMU Presidential Fellowship. N.M. thanks the Academy of Finland for funding (Grant No. 347775). I.N. and B.R. acknowledge funding from the European Research Council (Project No. 692891 DAMOCLES), the Academy of Finland flagship program (Grant No. 337549), the Centers of Excellence Program (CoE VILMA), and the University of Helsinki, Faculty of Science ATMATH project. N.M., I.N., and B.R. acknowledge the CSC-IT Center for Science in Espoo, Finland, for computational resources. The authors also thank Drs. Neil Donahue and Ranganathan Gopalakrishnan for their insights on ion−molecule interactions.

■ REFERENCES

(1) Merikanto, J.; Spracklen, D. V.; Mann, G. W.; Pickering, S. J.; Carslaw, K. S. Impact of Nucleation on Global CCN. *Atmospheric Chemistry and Physics* **2009**, *9* (21), 8601−8616.

(2) Gordon, H.; Kirkby, J.; Baltensperger, U.; Bianchi, F.; Breitenlechner, M.; Curtius, J.; Dias, A.; Dommen, J.; Donahue, N. M.; Dunne, E. M.; et al. Causes and Importance of New Particle Formation in the Present-Day and Preindustrial Atmospheres. *Journal of Geophysical Research: Atmospheres* **2017**, *122* (16), 8739−8760.

(3) Spracklen, D. V.; Carslaw, K. S.; Kulmala, M.; Kerminen, V.-M.; Sihto, S.-L.; Riipinen, I.; Merikanto, J.; Mann, G. W.; Chipperfield, M.; et al. P.; Wiedensohler, A.; et al. Contribution of Particle Formation to Global Cloud Condensation Nuclei Concentrations. *Geophys. Res. Lett.* **2008**, *35* (6), L06808.

(4) Wang, M.; Penner, J. E. Aerosol Indirect Forcing in a Global Model with Particle Nucleation. *Atmospheric Chemistry and Physics* **2009**, *9* (1), 239−260.

(5) Yu, F.; Luo, G. Simulation of Particle Size Distribution with a Global Aerosol Model: Contribution of Nucleation to Aerosol and CCN Number Concentrations. *Atmospheric Chemistry and Physics* **2009**, *9* (20), 7691−7710.

(6) Sipilä, M.; Berndt, T.; Petäjä, T.; Brus, D.; Vanhanen, J.; Stratmann, F.; Patokoski, J.; Mauldin, R. L.; Hyvärinen, A.-P.; Lihavainen, H.; et al. The Role of Sulfuric Acid in Atmospheric Nucleation. *Science* **2010**, *327*, 1243−1246.

(7) Cai, R.; Yan, C.; Yang, D.; Yin, R.; Lu, Y.; Deng, C.; Fu, Y.; Ruan, J.; Li, X.; Kontkanen, J.; et al. Sulfuric Acid-Amine Nucleation in Urban Beijing. *Atmospheric Chemistry and Physics* **2021**, *21* (4), 2457−2468.

(8) Weber, R. J.; McMurry, P. H.; Eisele, F. L.; Tanner, D. J. Measurement of Expected Nucleation Precursor Species and 3−500-Nm Diameter Particles at Mauna Loa Observatory, Hawaii. *Journal of the Atmospheric Sciences* **1995**, *52* (12), 2242−2257.

(9) Chen, M.; Titcombe, M.; Jiang, J.; Jen, C.; Kuang, C.; Fischer, M. L.; Eisele, F. L.; Siepmann, J. I.; Hanson, D. R.; Zhao, J.; et al. Acid-Base Chemical Reaction Model for Nucleation Rates in the Polluted Atmospheric Boundary Layer. *Proc. Natl. Acad. Sci. U. S. A.* **2012**, *109* (46), 18713−18718.

(10) Kirkby, J.; Curtius, J.; Almeida, J.; Dunne, E.; Duplissy, J.; Ehrhart, S.; Franchin, A.; Gagne, S.; Ickes, L.; Kurten, A.; et al. Role of Sulphuric Acid, Ammonia and Galactic Cosmic Rays in Atmospheric Aerosol Nucleation. *Nature* **2011**, *476*, 429−433.

(11) Jen, C. N.; McMurry, P. H.; Hanson, D. R. Stabilization of Sulfuric Acid Dimers by Ammonia, Methylamine, Dimethylamine, and Trimethylamine. *Journal of Geophysical Research: Atmospheres* **2014**, *119* (12), 7502−7514.

(12) Loukonen, V.; Kurtén, T.; Ortega, I. K.; Vehkamäki, H.; Pádua, A. A. H.; Sellegri, K.; Kulmala, M. Enhancing Effect of Dimethylamine in Sulfuric Acid Nucleation in the Presence of Water - a Computational Study. *Atmospheric Chemistry and Physics* **2010**, *10* (10), 4961−4974.

(13) Zhao, J.; Eisele, F. L.; Titcombe, M.; Kuang, C.; McMurry, P. H. Chemical Ionization Mass Spectrometric Measurements of Atmospheric Neutral Clusters Using the Cluster-CIMS. *J. Geophys. Res.* **2010**, *115*, D08205.

(14) Erupe, M. E.; Viggiano, A. A.; Lee, S. H. The Effect of Trimethylamine on Atmospheric Nucleation Involving H_2SO_4. *Atmos. Chem. Phys.* **2011**, *11*, 4767−4775.

(15) Zollner, J. H.; Glasoe, W. A.; Panta, B.; Carlson, K. K.; McMurry, P. H.; Hanson, D. R. Sulfuric Acid Nucleation: Power Dependencies, Variation with Relative Humidity, and Effect of Bases. *Atmos. Chem. Phys.* **2012**, *12*, 4399−4411.

(16) Lehtipalo, K.; Yan, C.; Dada, L.; Bianchi, F.; Xiao, M.; Wagner, R.; Stolzenburg, D.; Ahonen, L. R.; Amorim, A.; Baccarini, A.; et al. Multicomponent New Particle Formation from Sulfuric Acid, Ammonia, and Biogenic Vapors. *Science Advances* **2018**, *4* (12), No. eaau5363.

(17) Merikanto, J.; Napari, I.; Vehkamäki, H.; Anttila, T.; Kulmala, M. New Parameterization of Sulfuric Acid-Ammonia-Water Ternary

Nucleation Rates at Tropospheric Conditions. *Journal of Geophysical Research: Atmospheres* **2007**, *112*, D15207.
(18) Ortega, I. K.; Olenius, T.; Kupiainen-Määttä, O.; Loukonen, V.; Kurtén, T.; Vehkamäki, H. Electrical Charging Changes the Composition of Sulfuric Acid-Ammonia/Dimethylamine Clusters. *Atmos. Chem. Phys.* **2014**, *14*, 7995−8007.
(19) Sihto, S. L.; Kulmala, M.; Kerminen, V. M.; Dal Maso, M.; Petäjä, T.; Riipinen, I.; Korhonen, H.; Arnold, F.; Janson, R.; Boy, M.; et al. Atmospheric Sulphuric Acid and Aerosol Formation: Implications from Atmospheric Measurements for Nucleation and Early Growth Mechanisms. *Atmos. Chem. Phys.* **2006**, *6*, 4079−4091.
(20) Smith, J. N.; Draper, D. C.; Chee, S.; Dam, M.; Glicker, H.; Myers, D.; Thomas, A. E.; Lawler, M. J.; Myllys, N. Atmospheric Clusters to Nanoparticles: Recent Progress and Challenges in Closing the Gap in Chemical Composition. *J. Aerosol Sci.* **2021**, *153*, 105733.
(21) Almeida, J.; Schobesberger, S.; Kurten, A.; Ortega, I. K.; Kupiainen-Maatta, O.; Praplan, A. P.; Adamov, A.; Amorim, A.; Bianchi, F.; Breitenlechner, M.; et al. Molecular Understanding of Sulphuric Acid-Amine Particle Nucleation in the Atmosphere. *Nature* **2013**, *502*, 359−363.
(22) Elm, J.; Passananti, M.; Kurtén, T.; Vehkamäki, H. Diamines Can Initiate New Particle Formation in the Atmosphere. *J. Phys. Chem. A* **2017**, *121* (32), 6155−6164.
(23) Jen, C. N.; Bachman, R.; Zhao, J.; McMurry, P. H.; Hanson, D. R. Diamine-Sulfuric Acid Reactions Are a Potent Source of New Particle Formation. *Geophys. Res. Lett.* **2016**, *43*, 867−873.
(24) Olenius, T.; Halonen, R.; Kurtén, T.; Henschel, H.; Kupiainen-Määttä, O.; Ortega, I. K.; Jen, C. N.; Vehkamäki, H.; Riipinen, I. New Particle Formation from Sulfuric Acid and Amines: Comparison of Monomethylamine, Dimethylamine, and Trimethylamine. *J. Geophys. Res. Atmos.* **2017**, *122* (13), 7103−7118.
(25) Zhang, R.; Khalizov, A.; Wang, L.; Hu, M.; Xu, W. Nucleation and Growth of Nanoparticles in the Atmosphere. *Chem. Rev.* **2012**, *112* (3), 1957−2011.
(26) Elm, J.; Jen, C. N.; Kurtén, T.; Vehkamäki, H. Strong Hydrogen Bonded Molecular Interactions between Atmospheric Diamines and Sulfuric Acid. *J. Phys. Chem. A* **2016**, *120*, 3693−3700.
(27) Nadykto, A. B.; Herb, J.; Yu, F.; Xu, Y. Enhancement in the Production of Nucleating Clusters Due to Dimethylamine and Large Uncertainties in the Thermochemistry of Amine-Enhanced Nucleation. *Chem. Phys. Lett.* **2014**, *609*, 42−49.
(28) Lovejoy, E. R.; Curtius, J.; Froyd, K. D. Atmospheric Ion-Induced Nucleation of Sulfuric Acid and Water. *Journal of Geophysical Research: Atmospheres* **2004**, *109* (D8), D08204.
(29) Harrison, R. G.; Carslaw, K. S. Ion-Aerosol-Cloud Processes in the Lower Atmosphere. *Reviews of Geophysics* **2003**, *41* (3), 1012.
(30) Carslaw, K. S.; Harrison, R. G.; Kirkby, J. Cosmic Rays, Clouds, and Climate. *Science* **2002**, *298* (5599), 1732−1737.
(31) Duplissy, J.; Enghoff, M. B.; Aplin, K. L.; Arnold, F.; Aufmhoff, H.; Avngaard, M.; Baltensperger, U.; Bondo, T.; Bingham, R.; Carslaw, K.; et al. Results from the CERN Pilot CLOUD Experiment. *Atmospheric Chemistry and Physics* **2010**, *10* (4), 1635−1647.
(32) Talbot, R. W.; Mosher, B. W.; Heikes, B. G.; Jacob, D. J.; Munger, J. W.; Daube, B. C.; Keene, W. C.; Maben, J. R.; Artz, R. S. Carboxylic Acids in the Rural Continental Atmosphere over the Eastern United States during the Shenandoah Cloud and Photochemistry Experiment. *Journal of Geophysical Research: Atmospheres* **1995**, *100* (D5), 9335−9343.
(33) Chapman, E. G.; Kenny, D. V.; Busness, K. M.; Thorp, J. M.; Spicer, C. W. Continuous Airborne Measurements of Gaseous Formic and Acetic Acids over the Western North Atlantic. *Geophys. Res. Lett.* **1995**, *22* (4), 405−408.
(34) Grosjean, D. Organic Acids in Southern California Air: Ambient Concentrations, Mobile Source Emissions, in Situ Formation and Removal Processes. *Environ. Sci. Technol.* **1989**, *23* (12), 1506−1514.
(35) Khwaja, H. A. Atmospheric Concentrations of Carboxylic Acids and Related Compounds at a Semiurban Site. *Atmos. Environ.* **1995**, *29* (1), 127−139.
(36) Meng, Z.; Seinfeld, J. H.; Saxena, P. Gas/Aerosol Distribution of Formic and Acetic Acids. *Aerosol Sci. Technol.* **1995**, *23* (4), 561−578.
(37) Kawamura, K.; Ng, L. L.; Kaplan, I. R. Determination of Organic Acids (C1-C10) in the Atmosphere, Motor Exhausts, and Engine Oils. *Environ. Sci. Technol.* **1985**, *19* (11), 1082−1086.
(38) Staudt, M.; Wolf, A.; Kesselmeier, J. Influence of Environmental Factors on the Emissions of Gaseous Formic and Acetic Acids from Orange (Citrus Sinensis L.) Foliage. *Biogeochemistry* **2000**, *48* (2), 199−216.
(39) Kesselmeier, J. Exchange of Short-Chain Oxygenated Volatile Organic Compounds (VOCs) between Plants and the Atmosphere: A Compilation of Field and Laboratory Studies. *Journal of Atmospheric Chemistry* **2001**, *39* (3), 219−233.
(40) Rosado-Reyes, C. M.; Francisco, J. S. Atmospheric Oxidation Pathways of Acetic Acid. *J. Phys. Chem. A* **2006**, *110* (13), 4419−4433.
(41) Andreae, M. O.; Talbot, R. W.; Andreae, T. W.; Harriss, R. C. Formic and Acetic Acid over the Central Amazon Region, Brazil: 1. Dry Season. *Journal of Geophysical Research: Atmospheres* **1988**, *93* (D2), 1616−1624.
(42) Chebbi, A.; Carlier, P. Carboxylic Acids in the Troposphere, Occurrence, Sources, and Sinks: A Review. *Atmos. Environ.* **1996**, *30* (24), 4233−4249.
(43) Talbot, R. W.; Andreae, M. O.; Berresheim, H.; Jacob, D. J.; Beecher, K. M. Sources and Sinks of Formic, Acetic, and Pyruvic Acids over Central Amazonia: 2. Wet Season. *Journal of Geophysical Research* **1990**, *95* (D10), 16799−16811.
(44) Eisele, F. L.; McDaniel, E. W. Mass Spectrometric Study of Tropospheric Ions in the Northeastern and Southwestern United States. *Journal of Geophysical Research: Atmospheres* **1986**, *91* (D4), 5183−5188.
(45) Eisele, F. L. Natural and Anthropogenic Negative Ions in the Troposphere. *Journal of Geophysical Research: Atmospheres* **1989**, *94* (D2), 2183−2196.
(46) Perkins, M. D.; Eisele, F. L. First Mass Spectrometric Measurements of Atmospheric Ions at Ground Level. *Journal of Geophysical Research: Atmospheres* **1984**, *89* (D6), 9649−9657.
(47) Glasoe, W. A.; Volz, K.; Panta, B.; Freshour, N.; Bachman, R.; Hanson, D. R.; McMurry, P. H.; Jen, C. Sulfuric Acid Nucleation: An Experimental Study of the Effect of Seven Bases. *Journal of Geophysical Research: Atmospheres* **2015**, *120* (5), 1933−1950.
(48) Jen, C. N.; Zhao, J.; McMurry, P. H.; Hanson, D. R. Chemical Ionization of Clusters Formed from Sulfuric Acid and Dimethylamine or Diamines. *Atmos. Chem. Phys.* **2016**, *16* (19), 12513−12529.
(49) Veres, P.; Roberts, J. M.; Warneke, C.; Welsh-Bon, D.; Zahniser, M.; Herndon, S.; Fall, R.; de Gouw, J. Development of Negative-Ion Proton-Transfer Chemical-Ionization Mass Spectrometry (NI-PT-CIMS) for the Measurement of Gas-Phase Organic Acids in the Atmosphere. *Int. J. Mass Spectrom.* **2008**, *274*, 48−55.
(50) Berresheim, H.; Elste, T.; Plass-Dülmer, C.; Eisele, F. L.; Tanner, D. J. Chemical Ionization Mass Spectrometer for Long-Term Measurements of Atmospheric OH and H_2SO_4. *Int. J. Mass Spectrom.* **2000**, *202*, 91−109.
(51) Hanson, D. R.; Eisele, F. L. Measurement of Prenucleation Molecular Clusters in the NH_3, H_2SO_4, H_2O System. *J. Geophys. Res.* **2002**, *107*, 4158.
(52) Kürten, A.; Jokinen, T.; Simon, M.; Sipilä, M.; Sarnela, N.; Junninen, H.; Adamov, A.; Almeida, J.; Amorim, A.; Bianchi, F.; et al. Neutral Molecular Cluster Formation of Sulfuric Acid-Dimethylamine Observed in Real Time under Atmospheric Conditions. *Proc. Natl. Acad. Sci. U. S. A.* **2014**, *111*, 15019.
(53) Viggiano, A. A.; Perry, R. A.; Albritton, D. L.; Ferguson, E. E.; Fehsenfeld, F. C. Stratospheric Negative-Ion Reaction Rates with H2SO4. *J. Geophys. Res.* **1982**, *87*, 7340−7342.
(54) Viggiano, A. A.; Seeley, J. V.; Mundis, P. L.; Williamson, J. S.; Morris, R. A. Rate Constants for the Reactions of $XO_3^-(H_2O)_n$ (X = C, HC, and N) and $NO_3^-(HNO_3)_n$ with H_2SO_4: Implications for

https://doi.org/10.1021/acs.jpca.2c02072
J. Phys. Chem. A XXXX, XXX, XXX−XXX

Atmospheric Detection of H_2SO_4. *J. Phys. Chem. A* **1997**, *101*, 8275−8278.
(55) Fomete, S. K. W.; Johnson, J. S.; Myllys, N.; Jen, C. N. Experimental and Theoretical Study on the Enhancement of Alkanolamines on Sulfuric Acid Nucleation. *J. Phys. Chem. A* **2022**, *126* (25), 4057−4067.
(56) Fomete, S. K. W.; Johnson, J. S.; Casalnuovo, D.; Jen, C. N. A Tutorial Guide on New Particle Formation Experiments Using a Laminar Flow Reactor. *J. Aerosol Sci.* **2021**, *157*, 105808.
(57) Pfeifer, J.; Simon, M.; Heinritzi, M.; Piel, F.; Weitz, L.; Wang, D.; Granzin, M.; Müller, T.; Bräkling, S.; Kirkby, J.; et al. Measurement of Ammonia, Amines and Iodine Compounds Using Protonated Water Cluster Chemical Ionization Mass Spectrometry. *Atmospheric Measurement Techniques* **2020**, *13* (5), 2501−2522.
(58) Su, T.; Bowers, M. T. Ion-Polar Molecule Collisions. Effect of Molecular Size on Ion-Polar Molecule Rate Constants. *J. Am. Chem. Soc.* **1973**, *95* (23), 7609−7610.
(59) Kupiainen-Määttä, O.; Olenius, T.; Kurtén, T.; Vehkamäki, H. CIMS Sulfuric Acid Detection Efficiency Enhanced by Amines Due to Higher Dipole Moments: A Computational Study. *J. Phys. Chem. A* **2013**, *117*, 14109−14119.
(60) Heinritzi, M.; Simon, M.; Steiner, G.; Wagner, A. C.; Kürten, A.; Hansel, A.; Curtius, J. Characterization of the Mass-Dependent Transmission Efficiency of a CIMS. *Atmos. Meas. Technol.* **2016**, *9* (4), 1449−1460.
(61) Jen, C. N.; Zhao, J.; McMurry, P. H.; Hanson, D. R. Chemical Ionization of Clusters Formed from Sulfuric Acid and Dimethylamine or Diamines. *Atmos. Chem. Phys.* **2016**, *16* (19), 12513−12529.
(62) Su, T.; Bowers, M. T. Theory of Ion-polar Molecule Collisions. Comparison with Experimental Charge Transfer Reactions of Rare Gas Ions to Geometric Isomers of Difluorobenzene and Dichloroethylene. *J. Chem. Phys.* **1973**, *58*, 3027−3037.
(63) Su, T.; Su, E. C. F.; Bowers, M. T. Ion-Polar Molecule Collisions. Conservation of Angular Momentum in the Average Dipole Orientation Theory. The AADO Theory. *J. Chem. Phys.* **1978**, *69* (5), 2243−2250.
(64) Su, T.; Chesnavich, W. J. Parametrization of the Ion-Polar Molecule Collision Rate Constant by Trajectory Calculations. *J. Chem. Phys.* **1982**, *76* (10), 5183.
(65) Chesnavich, W. J.; Su, T.; Bowers, M. T. Collisions in a Noncentral Field: A Variational and Trajectory Investigation of Ion-Dipole Capture. *J. Chem. Phys.* **1980**, *72* (4), 2641−2655.
(66) Chai, J.-D.; Head-Gordon, M. Long-Range Corrected Hybrid Density Functionals with Damped Atom-Atom Dispersion Corrections. *Phys. Chem. Chem. Phys.* **2008**, *10* (44), 6615−6620.
(67) Eichelberger, B. R.; Snow, T. P.; Bierbaum, V. M. Collision Rate Constants for Polarizable Ions. *J. Am. Soc. Mass Spectrom.* **2003**, *14* (5), 501−505.
(68) Neefjes, I.; Halonen, R.; Vehkamäki, H.; Reischl, B. Modeling Approaches for Atmospheric Ion-Dipole Collisions: All-Atom Trajectory Simulations and Central Field Methods. *Atmospheric Chemistry and Physics* **2022**, *22* (17), 11155−11172.

https://doi.org/10.1021/acs.jpca.2c02072
J. Phys. Chem. A XXXX, XXX, XXX−XXX